JNS 2 (2012) 51-60

Journal of
NANOSTRUCTURES
JNS
NANOSTRUCTURES
JNS.kashanu.ac.ir

Numerical Study of Mixed Convection in a Lid-Driven Enclosure with a Centered Body Using Nanofluid Variable Properties

A. A. Abbasian*, G. A. Sheikhzadeh, R. Heidary, N. Hajialigol[*], M. Ebrahim-Qomi

Department of Mechanical Engineering, University of Kashan,Ghotb Ravandi Blvd, Kashan, 87317-51167, Iran.

Article history:
Received 11/8/2011
Accepted 20/4/2012
Published online 1/6/2012

Keywords:
Variable properties
Lid-driven enclosure
Mixed convection
Nanofluid
Enclosure with body.

**Corresponding author:*
E-mail address:
Najmeh.hajialigol@gmail.com

Abstract

In the present study, mixed convection laminar flow around an adiabatic body in a Lid-driven enclosure filled with nanofluid using variable thermal conductivity and variable viscosity is numerically investigated. The fluid around the body in the enclosure is a water-based nanofluid containing Al_2O_3 nanoparticles. The Vertical enclosure's walls are maintained at constant cold temperature and the horizontal bottom enclosure's wall is kept constant at hot temperature. Top enclosure's wall is insulated and moving with uniform velocity. The ratio of body's length to enclosure's length is kept constant at 1/3. The study has been carried out for the Richardson number of 0.01 to 100, the solid volume fraction of 0 to 0.06 and the Grashof number of 10^4. Various results for the streamlines and isotherms as well as the local and average Nusselt numbers are presented. By the use of variable properties in this study Interesting results are observed.

1. Introduction

Low thermal conductivity of conventional heat transfer fluids such as water, oil, and ethylene glycol mixture is a main limitation. Suspending small solid particles is a way to improve the heat transfer. Fluids with suspending nanoparticles are nanofluids, a term firstly used by Choi [1]. Among the numerous geometry studied in the heat transfer of nanofluids, the lid-driven enclosure has been a

Nomenclature

g	Gravitational acceleration	**Greek symbols**	
Gr	Grashof number	α	Thermal diffusivity
L	Enclosure length	β	Thermal expansion coefficient
Nu	Nusselt number	φ	Solid volume fraction
k	Thermal conductivity	μ	Dynamic viscosity
p	Pressure		Kinematics viscosity
P	Dimensionless pressure	ρ	Density
Pr	Prandtl number	θ	Dimensionless temperature
Ra	Rayleigh number	**Subscript**	
Re	Reynolds number	a	average
Ri	Richardson number	b	Bottom wall
T	Temperature	c	Cold wall
u, v	Components of velocity	eff	Effective
U, V	Dimensionless of velocity component	f	Fluid
U0	Velocity of the moving lid	h	Hot wall
W	Body length	l	Left wall
x, y	Cartesian coordinates	nf	Nanofluid
X, Y	Dimensionless of Cartesian coordinates	p	Particle
		r	Right wall

subject of interest in recent years due to its applications especially those related to lubrication technologies, electronic cooling, food processing and nuclear reactors [2-3]. Thus, many studies have been performed to investigate mixed convection in a lid-driven enclosure using a nanofluid. Mixed convection heat transfer is affected by nanofluid properties, such as viscosity and thermal conductivity. Most studies used the Brinkman model for the viscosity and Maxwell-Garnett (MG) model for the thermal conductivity. These models have some defects. In these models the effects of nanofluid temperature or nanoparticles size and also important mechanisms for heat transfer in nanofluids such as Brownian motion are not considered. The effect of nanoparticles concentration and nanoparticles size on nanofluids viscosity under a wide range of temperatures were experimentally studied by Nguyen et al. [5] And Angue Minsta et al. [6]. They found that viscosity decreases with increasing temperature, especially at high concentration of nanoparticles. In addition, Chon et al. [7] experimentally studied the combined effect of temperature, nanoparticle size and nanoparticles volume fraction on the thermal conductivity of nanofluids. Abu-Nada [8, 9] studied the effect of variable properties of Al_2O_3-water and CuO-water nanofluids on natural convection in an

annular region. The effect of variable properties on natural convection in a cavity filled with CuO-EG-Water nanofluid is investigated by Abu-Nada et al. [10]. Additionally, Abu-Nada et al. [11] investigated the role of nanofluid variable properties in differentially heated enclosures and found that the effect of nanofluid variable properties play a major role in the prediction of heat transfer enhancement. Mazrouei et al. [13] and Sheikhzadeh et al. [14] considered the effect of variable properties on mixed convection in a cavity filled with a nanofluid. The effects of an inserted body on natural and mixed convection in an enclosure have been investigated by several researchers. Natural convection in an enclosure with a conducting body is investigated by Lee et al. [15], Das et al. [16] and House et al. [17].

In the present study mixed convection around an adiabatic body in an enclosure filled with nanofluid using variable properties is investigated numerically. The effects of Richardson number and the solid volume fraction on isotherms and streamlines and average Nusselt numbers are presented.

2. Mathematical modeling

A schematic diagram of the enclosure with coordinate system and boundary conditions is shown in Fig.1. The Vertical enclosure's walls are maintained at constant cold temperature and the horizontal bottom enclosure's wall is kept constant at hot temperature. Top enclosure's wall is insulated and moving with uniform velocity.the ratio of W/L is maintained constant at 1/3 and the body is located in the center of the cavity. Al2O3-water nanofluid is used and it's thermophysical properties at T=25˚C is presented in Table.1. The nanofluid is considered Newtonian and incompressible and the nanofluid flow is assumed to be laminar.

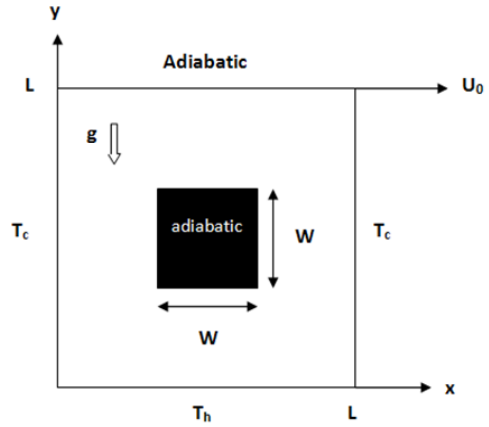

Fig. 1. Geometry and boundary conditions

Table 1. Thermophysical properties of water and Al_2O_3 **[7].**

Property	water	Al_2O_3
c_p	4179	765
ρ	997. 1	3970
k	0.6	25
β	2.1×10^{-4}	0.85×10^{-5}
d_p (nm)	0.384	47

The two dimensional continuity, momentum and energy equations for laminar mixed convection fluid flow and heat transfer with the Boussinesq approximation in y-direction are as following:

Continuity equation

$$\frac{\partial u}{\partial x}+\frac{\partial v}{\partial y}=0 \qquad (1)$$

x-momentum equation:

$$\rho_{nf,0}\left(u\frac{\partial u}{\partial x}+v\frac{\partial u}{\partial y}\right)=-\frac{\partial p}{\partial x}+\frac{\partial}{\partial x}\left(\mu_{nf}\frac{\partial u}{\partial x}\right)+\frac{\partial}{\partial y}\left(\mu_{nf}\frac{\partial u}{\partial y}\right)+\frac{\partial \mu_{nf}}{\partial y}\frac{\partial v}{\partial x}+\frac{\partial \mu_{nf}}{\partial x}\frac{\partial u}{\partial x} \qquad (2)$$

y-momentum equation:

$$\rho_{nf,0}\left(u\frac{\partial v}{\partial x}+v\frac{\partial v}{\partial y}\right)=-\frac{\partial p}{\partial y}+\frac{\partial}{\partial x}\left(\mu_{nf}\frac{\partial v}{\partial x}\right)+\frac{\partial}{\partial y}\left(\mu_{nf}\frac{\partial v}{\partial y}\right)+\frac{\partial\mu_{nf}}{\partial y}\frac{\partial v}{\partial y}+\frac{\partial\mu_{nf}}{\partial x}\frac{\partial u}{\partial y}+[\varphi\rho_{p,0}\beta_s+(1-\varphi)\rho_{f,0}\beta_f]g(T-T_c) \quad (3)$$

Energy equation:

$$(\rho c_p)_{nf}\left(u\frac{\partial T}{\partial x}+v\frac{\partial T}{\partial y}\right)=\frac{\partial}{\partial x}\left(k_{nf}\frac{\partial T}{\partial x}\right)+\frac{\partial}{\partial y}(k_{nf}\frac{\partial T}{\partial y}) \quad (4)$$

where the density, heat capacity, thermal expansion coefficient, and thermal diffusivity of the nanofluid are as following, respectively [4]:

$$\rho_{nf,0}=(1-\varphi)\rho_{f,0}+\varphi\rho_{p,0} \quad (5)$$

$$(\rho c_p)_{nf}=(1-\varphi)(\rho c_p)_f+\varphi(\rho c_p)_p \quad (6)$$

$$(\rho\beta)_{nf}=(1-\varphi)(\rho\beta)_f+\varphi(\rho\beta)_p \quad (7)$$

$$\alpha_{nf}=\frac{k_{nf}}{(\rho c_p)_{nf}} \quad (8)$$

The effective thermal conductivity of the nanofluid calculated by the Chon et al. model [7] is:

$$\frac{k_{nf}}{k_f}=1+64.7\varphi^{0.4076}\left(\frac{d_f}{d_p}\right)^{0.3690}\left(\frac{k_p}{k_f}\right)^{0.7476}Pr_T^{0.9955}\,Re^{1.2321} \quad (9)$$

Here Pr_T and Re are defined by:

$$Pr_T=\frac{\mu_f}{\rho_f\alpha_f} \quad (10)$$

$$Re=\frac{\rho_f k_b T}{3\pi\mu_f l_f} \quad (11)$$

$k_b=1.3807\times10^{-23}$ J/K, is the Boltzmann constant and l_f =0.17 nm is the mean path of fluid particles [7]. The viscosity of the nanoparticle (Al_2O_3) as given by Nguyen et al. [5] is:

$$\mu_{nf}=exp(3.003-0.04203T-0.5445\varphi+.00002553T^2+0.0524\varphi^2-1.622\varphi^{-1})\times10^{-3} \quad (12)$$

The temperature in Eq. (12) is expressed ^{0}C . The viscosity of the base fluid (water) is considered to change with temperature. The equation is used to obtain the viscosity of water [5]:

$$\mu_f=(1.2723\ln^5T-8.736\ln^4T+33.708\ln^3T-246.6\ln^2T+518.78\ln T+1153.9)\times10^{-6} \quad (13)$$

Using the dimensionless variables:

$$X=\frac{x}{H},Y=\frac{y}{H},U=\frac{u}{U_0},V=\frac{v}{U_0},P=\frac{p}{\rho_f{U_0}^2},\theta=\frac{T-T_c}{T_h-T_c}$$

the governing equations are written in the dimensionless form:

Continuity equation

$$\frac{\partial U}{\partial X}+\frac{\partial V}{\partial Y}=0 \quad (14)$$

x-momentum equation:

$$U\frac{\partial U}{\partial X}+V\frac{\partial U}{\partial Y}=-\frac{\rho_{f,0}}{\rho_{nf,0}}\frac{\partial P}{\partial X}+\frac{1}{Re\times\vartheta_f\times\rho_{nf,0}}[\frac{\partial}{\partial X}\left(\mu_{nf}\frac{\partial U}{\partial X}\right)+\frac{\partial}{\partial Y}\left(\mu_{nf}\frac{\partial U}{\partial Y}\right)+\left(\frac{\partial\mu_{nf}}{\partial Y}\frac{\partial V}{\partial X}+\frac{\partial\mu_{nf}}{\partial X}\frac{\partial U}{\partial X}\right)] \quad (15)$$

y-momentum equation:

$$U\frac{\partial V}{\partial X}+V\frac{\partial V}{\partial Y}=-\frac{\rho_{f,0}}{\rho_{nf,0}}\frac{\partial P}{\partial Y}+\frac{1}{Re\times\vartheta_f\times\rho_{nf,0}}[\frac{\partial}{\partial X}\left(\mu_{nf}\frac{\partial V}{\partial X}\right)+\frac{\partial}{\partial Y}\left(\mu_{nf}\frac{\partial V}{\partial Y}\right)+\left(\frac{\partial\mu_{nf}}{\partial Y}\frac{\partial V}{\partial Y}+\frac{\partial\mu_{nf}}{\partial X}\frac{\partial U}{\partial Y}\right)]+\frac{(\rho\beta)_{nf}}{\beta_f\rho_{nf,0}}Ri\theta \quad (16)$$

Energy equation:

$$U\frac{\partial\theta}{\partial X}+V\frac{\partial\theta}{\partial Y}=\frac{1}{Re\times Pr\times\alpha_f\times(\rho c_p)_{nf}}\left[\frac{\partial}{\partial X}\left(K_{nf}\frac{\partial\theta}{\partial X}\right)+\frac{\partial}{\partial Y}\left(K_{nf}\frac{\partial\theta}{\partial Y}\right)\right] \quad (17)$$

The Grashohf, Reynolds, Richardson and Prandtl numbers in the above equations are defined as:

$$Gr=\frac{g\beta H^3(T_h-T_c)}{{\vartheta_f}^2},\quad Re=\frac{U_0H}{\vartheta_f},\quad Ri=\frac{Gr}{Re^2},\quad Pr=\frac{\vartheta_f}{\alpha_f} \quad (18)$$

The Nusselt number on the hot wall is calculated as follows:

$$Nu = \frac{-k_{nf}}{k_f}\frac{\partial\theta}{\partial Y}\Big|_{Y=0} \quad (19)$$

Finally, the average Nusselt number on the bottom wall is determined from:

$$Nu_a = \int_0^1 Nu(X)dX \quad (19)$$

3. Numerical method

The governing equations associated with the boundary conditions are solved numerically using the control-volume based finite volume method. The SIMPLE algorithm is used to solve the coupled system of governing equations. The under-relaxation factors for U-velocity, V-velocity and energy equations are 0.7, 0.7 and 0.9 respectively. A uniform grid mesh is employed in the present paper and the grid size of 141×141 is adequately appropriate to ensure a grid independent solution (Fig.2). The model is validated via several test problems [14]. Also, Fig. 3 presents comparison between the present work and the results of Lee et al. [15]. It is obvious that results are in good agreement.

4. Results and discussion

The fluid inside the enclosure is Al_2O_3-water nanofluid. To study the effects of the flow regime, the Richardson number of 0.01- 100, volume fraction of 0 -0.06 and Grashof number of $Gr=10^4$ is considered. Richardson number represents the ratio of natural convection strength to forced convection (Gr/Re^2). Reynolds number varies due to variation of Richardson number. The results are presented in the forms of isotherms and streamlines plots. Figs.4 and 5 show isotherms and streamlines plots of Ri= 0.01 and 0.1. At Ri=0.01 and Ri=0.1 forced convection is dominant. It is observed from Figs.4 and 5 that due to moving the fluid with the lid, secondary vortices cover the vacuum at the right top corner of the body.

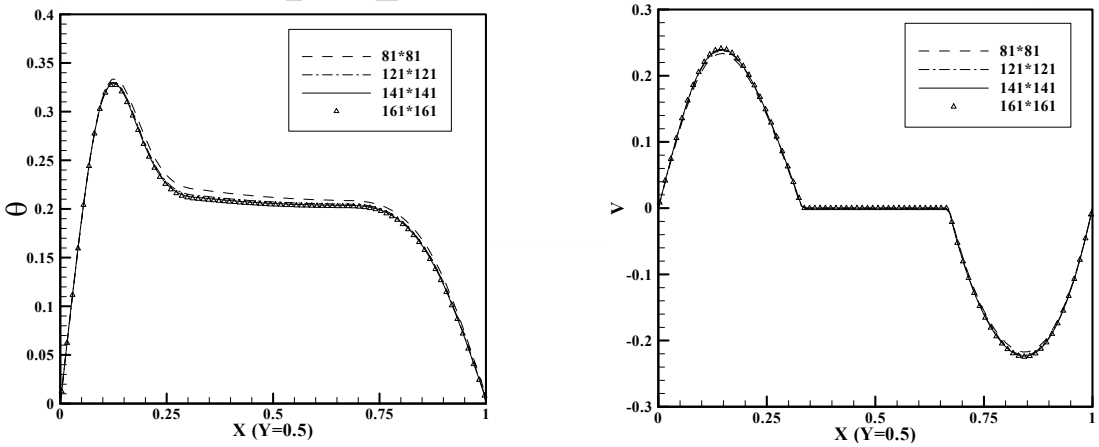

Fig. 2. Grid independency

Fig. 3. The comparison between Isotherms for adiabatic body at Ra=10^3(left) and 10^4(right) Lee(solid lines) [15], present work(dashed line).

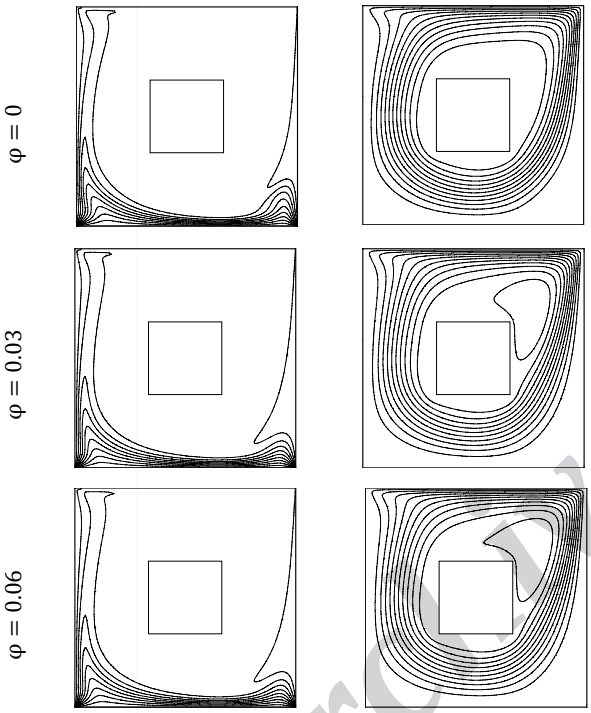

Fig. 4. Streamlines (right) and isotherms (left) for Al_2O_3-water nanofluid at Ri=0.01.

By increasing the Richardson number from 0.01 to 0.1 the effect of forced convection decreases and secondary vortices move to the top of the body. Isotherms show that by increasing Richardson number to 0.1 thermal boundary layer moves from the vertical walls to center of the enclosure. Increase of volume fraction makes densser isotherm lines at the bottom wall.

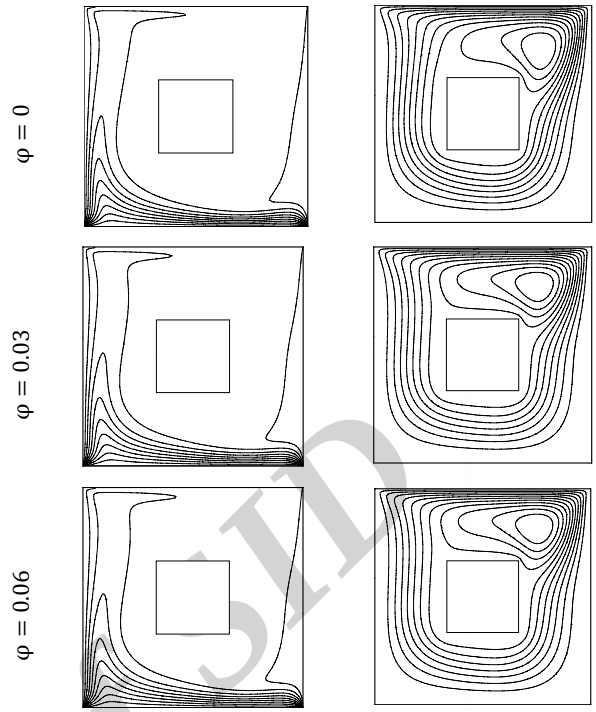

Fig. 5:Streamlines (right) and isotherms (left) for Al_2O_3-water nanofluid at Ri=0. 1.

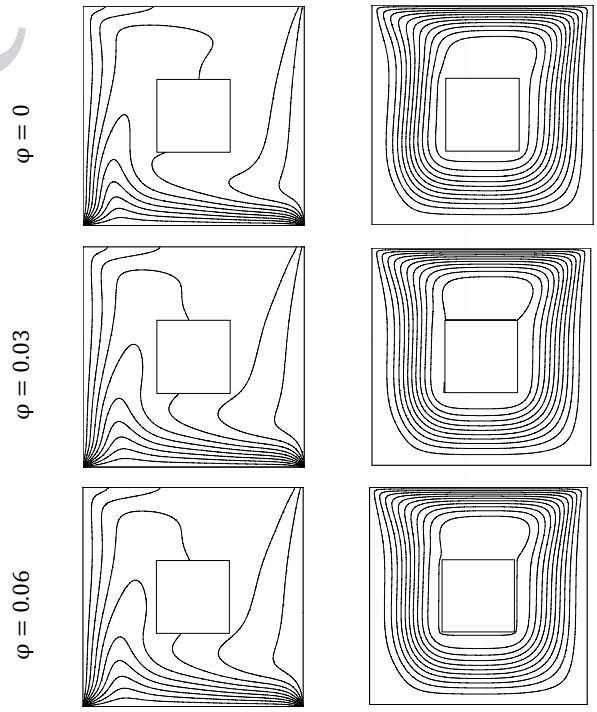

Fig. 6. Streamlines (right) and isotherms (left) for Al_2O_3-water nanofluid at Ri=10.

According to Figs.6 and 7, at Ri=10 and Ri=100, natural convection is much more effective than forced convection. It is obviously recognized from these figures, when forced convection is governed, the effect of increasing volume fraction of nanoparticles is prominent. If there is not body at the center, two large vortices cover the enclosure [18].

Clockwise vortex at the right and countor clockwise at the left of the enclosure. At Fig.7 natural convection causes to appear a weak vortex at the left of the body. By increasing the volume fraction to 0.06 this weak vortex moves to bottom.

Fig.8 shows the horizontal velocity at the midplane of the enclosure at various Richardson numbers. It is observed that by increasing the volume fraction, the horizontal velocity decreases. The reason is that nanoparticles make the nanofluid densser than the base fluid and it causes nanofluid to move hard.

At Ri=100 because of the dominated natural convection, U-velocity is increased at the bottom of the body while Forced convection dominated flow (Ri=0.01) has weak effect on the bottom of the body.

Fig. 9 shows local Nusselt number along the heated wall at various Richardson number at three volume fraction of 0, 0.03, 0.06. It is observed that by increasing the volume fraction to 0.06 strength of heat transfer increases.

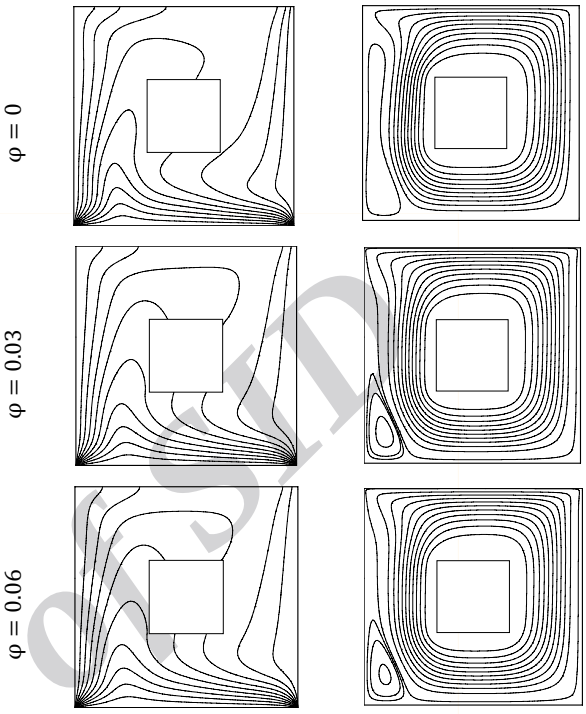

Fig. 7. Streamlines (right) and isotherms (left) for Al_2O_3-water nanofluid at Ri=100.

Average Nusselt number on the hot wall is presented at Fig. 10. It is observed that by increasing the volume fraction, average Nusselt number increases by decreasing the Richardson number to 0.01 heat transfer increases (Fig. 10). Because of the forced dominant convection at Ri = 0.01, there is maximum heat transfer at this value.

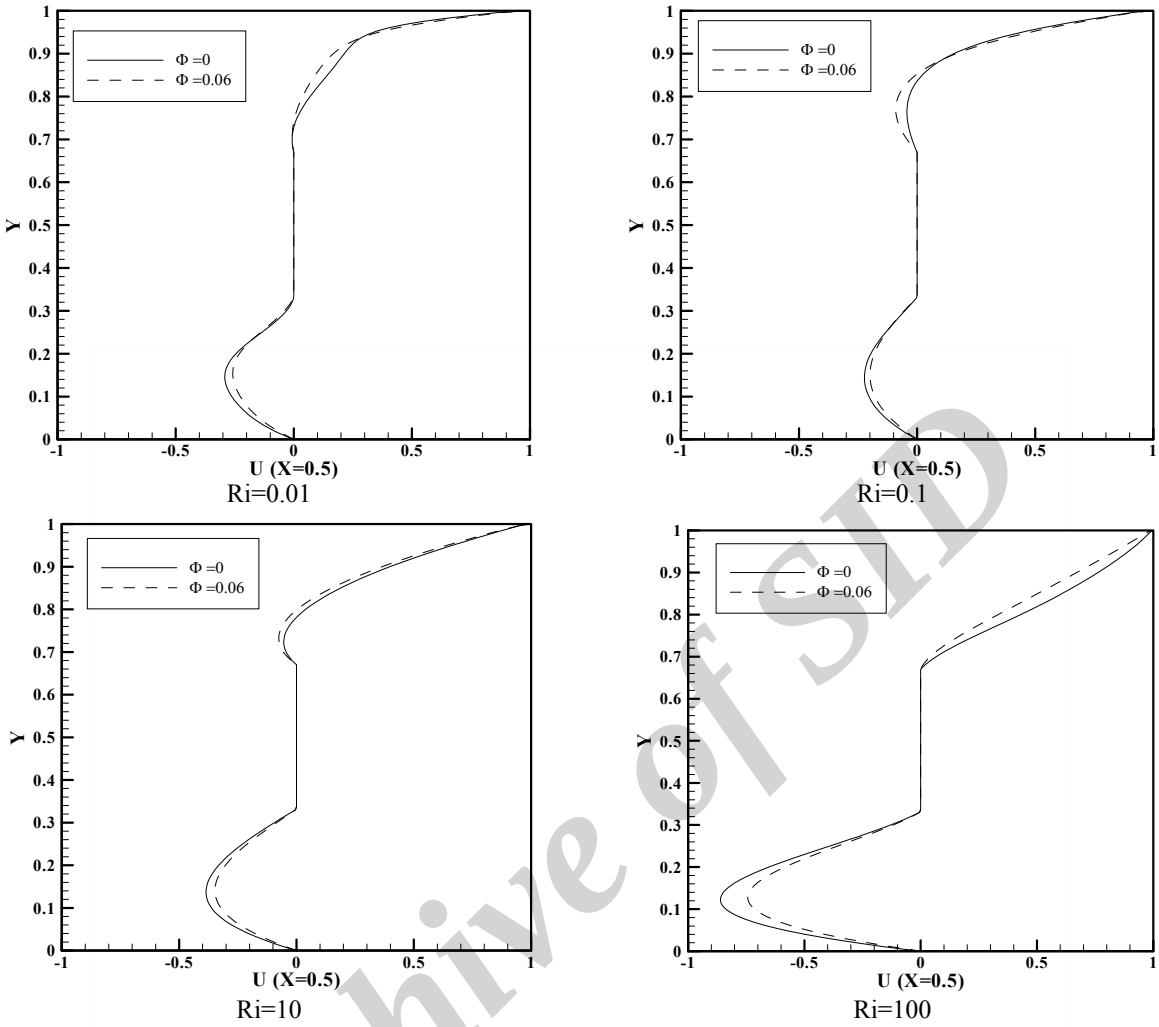

Fig. 8. Comparison U- velocity at the mid-plane of the cavity for base fluid and nanofluid at various Ri.

5. Conclusions

In this study, Laminar mixed convection flow of Al_2O_3–water nanofluid in a square enclosure around an adiabatic body were numerically investigated using variable thermal conductivity and variable viscosity propertiese. For the effective thermal conductivity of the nanofluid the model of Chon et al. [7] and for viscosity of the water-based and nanofluid the model of Nguyen et al. [5] is used effects of Richardson number and volume fraction at constant Grashof of 10^4 is considered. Results indicated that when forced convection was governed, the effect of increasing volume fraction of nanoparticles was more prominent. It was observed that by increasing the volume fraction, the horizontal velocity decreased. Also results showed that average Nusselt number increased by increasing the volume fraction of nanoparticles and reduction of Richardson number.

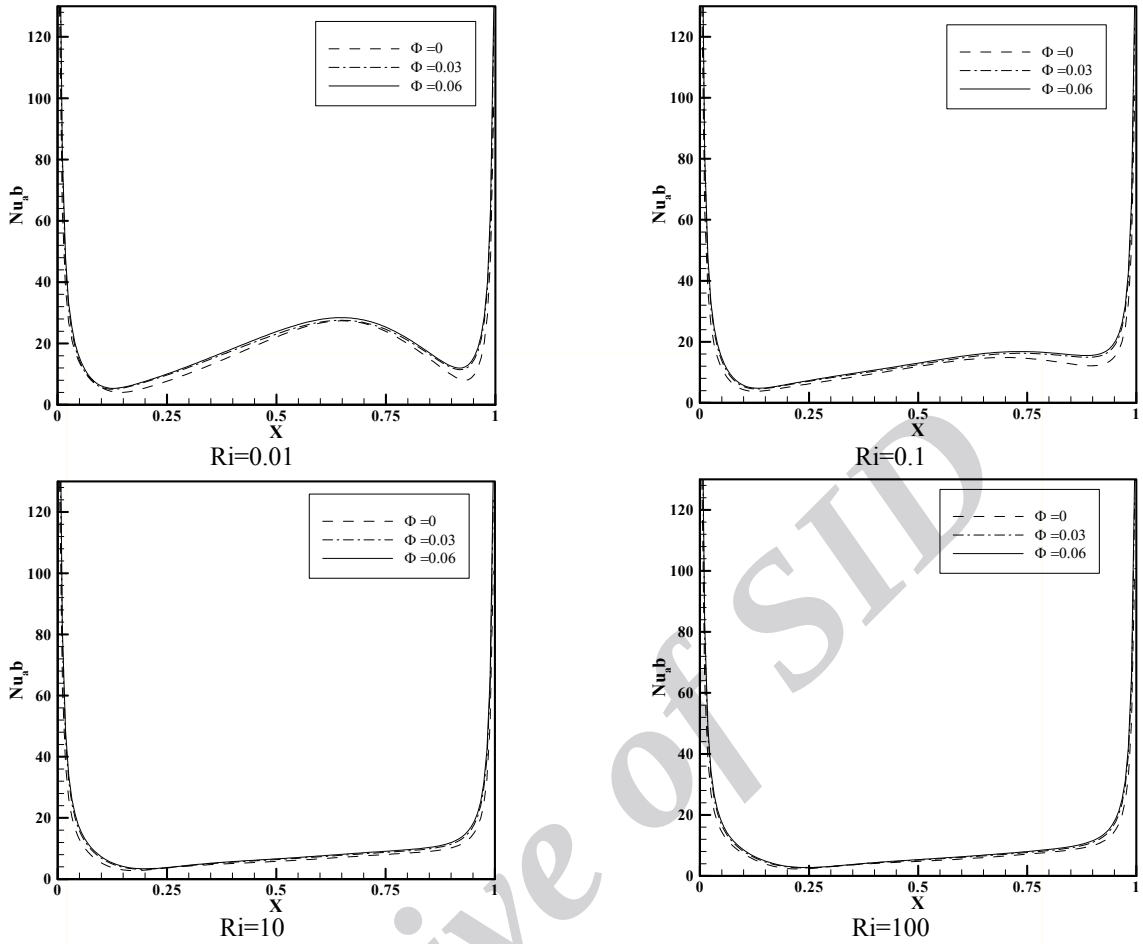

Fig. 9. Local Nusselt number distribution along the heated surface.

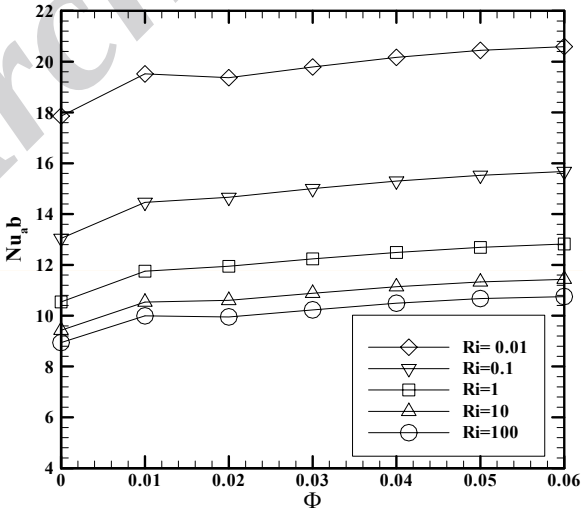

Fig. 10. Average Nusselt number on the bottom wall of the enclosure versus volume fraction at various Richardson number.

References

[1] U.S. Choi, ASME Fluids Eng. Div. 231 (1995) 99-105.

[2] J.R. Koseff, A.K. Prasad, J. Fluids Eng. Transactions of the ASME106 (1984) 390-398.

[3] M. Morzinski, C.O. Popiel, Num. Heat Trans. 12 (1988) 265-273.

[4] K. Khanafer, K. Vafai, M. Lightstone, Int. J. Heat Mass Tran. 46 (2003) 3639-3653.

[5] C.T. Nguyen, F. Desgranges, G. Roy, N. Galanis, T. Mare, S. Boucher, H. Angue Minsta, Int. J. Heat Fluid Flow 28 (2007) 1492–1506.

[6] H. Angue Minsta, G. Roy, C.T. Nguyen, D. Doucet, Int. J. Therm. Sci. 48 (2) (2009) 363–371.

[7] C.H. Chon, K.D. Kihm, S.P. Lee, S.U.S. Choi, Appl. Phys. Lett. 87 (2005) 153107.

[8] E. Abu-Nada, Int. J. Heat Fluid Flow 30 (2009) 679–690.

[9] E. Abu-Nada, ASME J. Heat Transfer, in press, (2010) DOI: 10.1115/1.4000440.

[10] Eiyad Abu-Nada a, Ali J. Chamkha, Int. J. Thermal Sci. 49 (2010) 2339-2352.

[11] E. Abu-Nada, Z. Masoud, H. Oztop, A. Campo, Int. J. Thermal Sci. 49 (2010) 479-491.

[12] H.F. Oztop, E. Abu-Nada, Int. J. Heat Fluid Flow 29 (2008) 1326–1336.

[13] Saeed Mazrouei Sebdani, Mostafa Mahmoodi, Seyed Mohammad Hashemi, Int. J. Thermal Sci. (2011) 1-15, DOI:10.1016/j.ijthermalsci.2011.09.003.

[14] G.A. Sheikhzadeh, M. Ebrahim Qomi, N. Hajialigol, A. Fattahi, Results Phys (2012), DOI:10.1016/j.rinp.2012.01.001.

[15] Jae Ryong Lee, Man Yeong Ha, Int. J. Heat and Mass Transfer 48 (2005) 3308–3318.

[16] Manab Kumar Das, K. Saran Kumar Reddy, Int. J. Heat and Mass Transfer 49 (2006) 4987–5000.

[17] John M. House, Christoph Beckermann and Theodore F. Smith, Effect, Int. J. Computation and Methodology, (1990) 18:2, 213-225.

[18] Tanmay Basak, S.Roy, Pawan Kumar Sharma, I. Pop, International Journal of Thermal Sciences 48 (2009) 891–912.